Langmuir
Article
pubs.acs.org/Langmuir

Characterization of Streptavidin Binding to Biotinylated, Binary Self-Assembled Thiol Monolayers—Influence of Component Ratio and Solvent

Michael Seifert,[†] Matthias T. Rinke,[‡] and Hans-Joachim Galla*,[†]

[†]*Institute of Biochemistry, University of Muenster, Wilhelm-Klemm-Strasse 2, 48149 Muenster, Germany, and* [‡]*Institute of Physical Chemistry, University of Muenster, Corrensstrasse 28/30, 48149 Muenster, Germany*

Received October 27, 2009. Revised Manuscript Received January 28, 2010

Many biosensor applications are based on streptavidin (SA) binding to partially biotinylated self-assembled thiol monolayers (SAMs). In our study, binary SAMs on gold were prepared from solutions containing 16-mercapto-1-hexadecanol (thiol I) and *N*-(8-biotinyl-3,6-dioxa-octanamidyl)-16-mercaptohexadecanamide (thiol II) in varying component ratios. Either chloroform or ethanol was used as solvent. After 24 h thiol incubation, SA was immobilized on the resulting SAMs using the strong SA-biotin interaction. The SA binding process was monitored by QCM-D (quartz crystal microbalance monitoring dissipation factor). It is shown that the Sauerbrey equation is valid to calculate the mass quantities of the immobilized SA layers. Under the chosen incubation conditions, marginal fractions of the biotinylated component II in chloroform ($(n_I/n_{II})_{solution} \approx 1000$) lead to SAMs which ensure a maximal SA binding quantity of $m_{Sauerbrey\ SA} \approx 400\ ng \cdot cm^{-2}$, being equivalent to a SA single-layer arrangement on the SAM surface. In case of incubations from ethanolic solutions, a complete SA layer formation needs significantly higher amounts of the biotinylated component II during SAM preparation ($(n_I/n_{II})_{solution} \approx 50$). X-ray photoelectron spectroscopy data show that the fraction of biotinylated thiol II in the SAM determines the amount of surface-bound SA. The SAM thiol ratio ($(n_I/n_{II})_{SAM}$) not only depends on the corresponding component ratio in the incubation solution, but is also strongly influenced by the solvent. Using chloroform as solvent during SAM preparation significantly increased the fraction of biotinylated thiol II in the SAMs compared to ethanol.

Introduction

Within current biotechnology research, one major emphasis lies in adequate biochip development for monitoring interactions and functions of biologically active molecules in a high-throughput and reproducible manner.[1−3] Nowadays, these systems gain broad application in analysis of environmental pollutants,[4] expression profiling,[5] or medical diagnostics.[6]

A general feature of such biosensors are noble metal[7] or silica[8] surfaces as solid supports to connect the corresponding biomolecule to a transducer based on, e.g., piezoelectric,[9] spectroscopic,[10] electrochemical,[11] or optical[12] techniques. The application of all these surface-sensitive analytical tools demands an interface between an inorganic substrate and a biological system. Without appropriate modification of the transducer surface, the biomolecules are immobilized in non-native, unknown conformational orientation,[13] often unspecifically bound. Such a disordered arrangement may lead to a decreased biological function and altered structural properties.

One strategy to obtain compatibility of inorganic and biological components is the use of the well-known streptavidin−biotin (SA-biotin) interaction exhibiting an extremely high binding constant ($K_a \approx 10^{13}\ M^{-1}$).[14] The SA protein with its four equivalent binding pockets for biotin[6] can be used as connecting entity between a prefunctionalized, biotinylated transducer surface and the (also prebiotinylated) biological component of interest. In many cases, this assembly can be established without noticeable impact on function and activity of the biomolecule.[15]

In the case of noble metal transducers (e.g., gold substrates), the biotinylation of the inorganic surface is often accomplished by constitution of self assembled monolayers (SAMs) composed of alkanethiols, partially functionalized with biotin. A great benefit of these SAMs in comparison to, e.g., surface functionalization by spreading of biotin doped liposomes, is the relatively easy preparation and long-term stability/functionality.[7] In the case of rather long alkyl chains, hydrophobic forces among the chemisorbed thiols lead to highly organized monolayers, which completely shield the hydrophilic metal surface.[16] The physicochemical character of the surface of the sensor system is exclusively determined by the SAM molecules and their different headgroup modifications.[17,18] SAMs for subsequent SA immobilization

*Corresponding author. Hans-Joachim Galla. Mailing address: Institute of Biochemistry, Wilhelm-Klemm-Strasse 2, 48149 Muenster, Germany. Phone: 0049/251-833200. Fax: 0049/251-8333206. E-mail: gallah@uni-muenster.de.

(1) Tanaka, M.; Sackmann, E. *Nature* **2005**, *437*, 656.
(2) Schaferling, M.; Riepl, M.; Pavlickova, P.; Paul, H.; Kambhampati, D.; Liedberg, B. *Microchim. Acta* **2003**, *142*, 193.
(3) Su, X. D.; Wu, Y. J.; Robelek, R.; Knoll, W. *Langmuir* **2005**, *21*, 348.
(4) Helali, S.; Ben Fredj, H.; Cherif, K.; Abdelghani, A.; Martelet, C.; Jaffrezic-Renault, N. *Mater. Sci. Eng. C* **2008**, *28*, 588.
(5) Schena, M.; Shalon, D.; Heller, R.; Chai, A.; Brown, P. O.; Davis, R. W. *Proc. Natl. Acad. Sci. U.S.A.* **1996**, *93*, 10614.
(6) Grunwald, C. *Z. Phys. Chem.* **2008**, *222*, 789.
(7) Love, J. C.; Estroff, L. A.; Kriebel, J. K.; Nuzzo, R. G.; Whitesides, G. M. *Chem. Rev.* **2005**, *105*, 1103.
(8) Mehne, J.; Markovic, G.; Proll, F.; Schweizer, N.; Zorn, S.; Schreiber, F.; Gauglitz, G. *Anal. Bioanal. Chem.* **2008**, *391*, 1783.
(9) Larsson, C.; Rodahl, M.; Hook, F. *Anal. Chem.* **2003**, *75*, 5080.
(10) Pradier, C. M.; Salmain, M.; Liu, Z.; Methivier, C. *Surf. Interface Anal.* **2002**, *34*, 67.
(11) Hays, H. C. W.; Millner, P. A.; Prodromidis, M. I. *Sens. Actuators B* **2006**, *114*, 1064.
(12) Reimhult, E.; Larsson, C.; Kasemo, B.; Hook, F. *Anal. Chem.* **2004**, *76*, 7211.
(13) Ladd, J.; Boozer, C.; Yu, Q. M.; Chen, S. F.; Homola, J.; Jiang, S. *Langmuir* **2004**, *20*, 8090.
(14) Green, N. M. *Adv. Protein Chem.* **1975**, *29*, 85.
(15) Jung, L. S.; Nelson, K. E.; Stayton, P. S.; Campbell, C. T. *Langmuir* **2000**, *16*, 9421.
(16) Bain, C. D.; Troughton, E. B.; Tao, Y. T.; Evall, J.; Whitesides, G. M.; Nuzzo, R. G. *J. Am. Chem. Soc.* **1989**, *111*, 321.
(17) Bain, C. D.; Evall, J.; Whitesides, G. M. *J. Am. Chem. Soc.* **1989**, *111*, 7155.

are often composed of binary thiol mixtures, one biotinylated, one terminated with a so-called spacer or diluent function like hydroxyl[19−22] or oligoethylene glycol[15,23,24] groups. The biotin functions protrude from the surface being accessible for specific SA linkage,[22] whereas the diluent function prevents unspecific binding.[20,25] The protrusion effect is enhanced by insertion of oligoethylene glycol spacers between the alkyl chain and the biotin function, ensuring flexibility of the linker unit. The precise fraction of biotinylated thiol needed for maximal SA binding seems to depend on structural properties like alkyl chain length and/or headgroup character.[15,20,24,26] Even marginal structural variations might be responsible for changes in SAM surface texture, resulting in differing SA immobilization quantities.[26] In addition, the thiol ratio in the SAMs often deviates from the component ratio in the incubation solution, since chemisorption efficiency depends on both the structural properties of the corresponding constituent and the solvent used during SAM formation.[17,24,27]

In the present study, we focus on preparation and analysis of partially biotinylated binary SAMs composed of a hydroxyl functionalized diluent component (16-mercapto-1-hexadecanol, thiol I) and a biotinylated one (*N*-(8-biotinyl-3,6-dioxa-octanamidyl)-16-mercaptohexadecanamide, thiol II) (Figure 1). For SAM formation, we used chloroform and ethanol as incubation solvent. Thiol SAM ratios ($(n_I/n_{II})_{SAM}$) and subsequent SA immobilization capacities were determined by QCM-D (quartz crystal microbalance monitoring dissipation factor[3,9,28,29] and XPS (X-ray photoelectron spectroscopy) analysis. We will show that the SA adsorption efficiency depends on the thiol SAM ratio $(n_I/n_{II})_{SAM}$ and that $(n_I/n_{II})_{SAM}$ is strongly influenced by the choice of thiol solvent during SAM formation.

Experimental Section

Materials. 16-Mercaptohexadecanoic acid/90% (Sigma-Aldrich/GER), 2,2-(ethylenedioxy)bis-(ethylamine) (Aldrich/GER), biotin (Sigma/GER), *O*-(*N*-succinimidyl)-*N*,*N*,*N*′,*N*′-tetramethyl-uroniumtetrafluoroborate (TSTU) (Fluka/GER), *N*,*N*-diisopropylethylenamine (DIPEA) (Sigma-Aldrich/GER), *N*-hydroxysuccinimide (NHS) (Aldrich/GER), and *N*,*N*′-dicyclohexylcarbodiimide (DCC) (Aldrich/GER) were used for synthesis of *N*-(8-biotinyl-3,6-dioxa-octanamidyl)-16-mercaptohexadecanamide (thiol II). 16-Mercapto-1-hexadecanol/99% (thiol I) (Frontier Scientific Europe Ltd., UK) was used without further purification. Chloroform and ethanol in HPLC grade (Merck/GER) were applied as organic solvents for thiol incubations. Ammoniac solution (25%) and hydroxyperoxide (30%) for gold substrate cleaning were purchased from Merck/GER. Water for SAM rinsing and buffer preparation was purified and deionized by a Millipore multicartridge system (Billerica/USA). TBS buffer

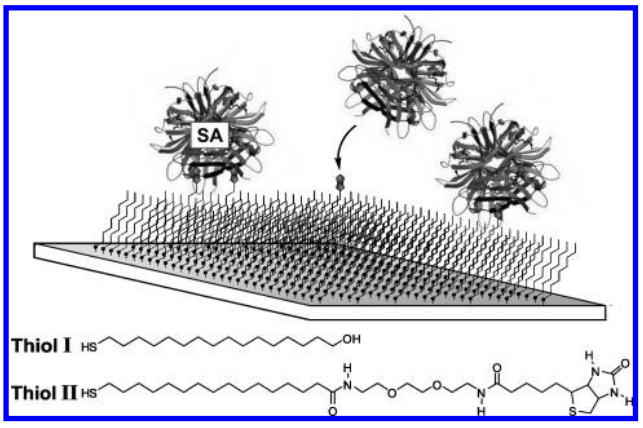

Figure 1. Schematic view of a binary thiol SAM (thiol components I and II) on gold. SA may bind to one or two protruding biotin moieties. (SA crystal structure was taken from RCSB Protein Data Bank (www.rcsb.org)).

(0.02 M tris(hydroxymethyl)aminomethane (tris base) (Sigma/GER), 0.1 M sodium chloride (NaCl) (AppliChem) in water) was adjusted to pH 7.4 by hydrochloric acid (p.a.). Streptavidin (M_{SA} ≈ 55 kDa) (Rockland/USA) was received in the form of lyophilized powder (from 0.15 M NaCl in water). Storage was conducted at −20 °C after restoring in water (1 mg/mL, 0.1 mL aliquots. Thawed stock solutions were stored at 4 °C for several weeks without further freeze/thaw cycles. Diluted Mucasol (Merz/GER) (5 mL/L water) was used as detergent for gold substrate cleaning. Gold surfaces applied for XPS measurements were prepared with Tempax glass slides (Rettberg/GER), chromium (Bal Tec/FL), and gold (Degussa/GER). QCM-D analysis was accomplished by using commercially available AT-cut quartz crystals (QSX 301-Standard Gold from Q-Sense/Sweden).

Synthesis of Thiol II. *N*-(8-Biotinyl-3,6-dioxa-octanamidyl)-16-mercaptohexadecanamide (Figure 1) was synthesized by a combination of former developed synthesis pathways in a three step synthesis.[26,30,31] Biotin was in situ activated by TSTU/DIPEA and directly coupled to dropwise added 2,2′-(ethylenedioxy)-bis(ethylamine) (step 1). The carboxylic acid function of 16-mercaptohexadecanoic acid was activated for amine coupling by NHS/DCC (step 2). A crucial advantage of the gentle NHS/DCC method in comparison to TSTU coupling procedure lies in preserving the free thiol function. Using the very fast and efficient[30] (and thus less selective) TSTU pathway resulted in irreversible bonding between the free thiol function and the carbodiimide derivative fragment of TSTU.

Using DCC, previous protection (and final deprotection) of the thiol function could be avoided, leading to a more straightforward synthesis pathway. In a last step (step 3), the NHS-activated 16-mercaptohexadecanoic acid was coupled to the biotinylated amine resulting in thiol II for SAM formation.

SAM Preparation. Thiol SAMs were constructed on either QSX 301-Standard Gold AT-cut quartz crystals (QCM-D measurements) or self-made gold supports (XPS analysis). The in-house fabricated gold layers were arranged by consecutive deposition of a 2 nm chromium adhesion layer and a 100-nm-thick gold layer on extensively purified glass slides of (0.5−1) cm^2 size. A detailed description can be found elsewhere.[32] All gold supports were precleaned in 5/1/1 water/ammoniac solution (25%)/hydroxyperoxide (30%) (volume ratio) for 5 min at 80 °C. Accurate purification was reached by consecutive washing with detergent solution (Mucasol) and water at 50 °C for 15 min in each case. After drying in a nitrogen stream, the substrates were

(18) Bain, C. D.; Whitesides, G. M. *J. Am. Chem. Soc.* **1989**, *111*, 7164.
(19) Yao, D. F.; Kim, J.; Yu, F.; Nielsen, P. E.; Sinner, E. K.; Knoll, W. *Biophys. J.* **2005**, *88*, 2745.
(20) Perez-Luna, V. H.; O'Brien, M. J.; Opperman, K. A.; Hampton, P. D.; Lopez, G. P.; Klumb, L. A.; Stayton, P. S. *J. Am. Chem. Soc.* **1999**, *121*, 6469.
(21) Stengel, G.; Hook, F.; Knoll, W. *Anal. Chem.* **2005**, *77*, 3709.
(22) Azzaroni, O.; Mir, M.; Knoll, W. *J. Phys. Chem. B* **2007**, *111*, 13499.
(23) Jung, L. S.; Nelson, K. E.; Campbell, C. T.; Stayton, P. S.; Yee, S. S.; Perez-Luna, V.; Lopez, G. P. *Sens. Actuators B* **1999**, *54*, 137.
(24) Nelson, K. E.; Gamble, L.; Jung, L. S.; Boeckl, M. S.; Naeemi, E.; Golledge, S. L.; Sasaki, T.; Castner, D. G.; Campbell, C. T.; Stayton, P. S. *Langmuir* **2001**, *17*, 2807.
(25) Ostuni, E.; Chapman, R. G.; Holmlin, R. E.; Takayama, S.; Whitesides, G. M. *Langmuir* **2001**, *17*, 5605.
(26) Riepl, M.; Enander, K.; Liedberg, B.; Schaferling, M.; Kruschina, M.; Ortigao, F. *Langmuir* **2002**, *18*, 7016.
(27) Xing, Y. F.; Li, S. F. Y.; Lau, A. K. H.; O'Shea, S. J. *J. Electroanal. Chem.* **2005**, *583*, 124.
(28) Rodahl, M.; Hook, F.; Kasemo, B. *Anal. Chem.* **1996**, *68*, 2219.
(29) Rodahl, M.; Kasemo, B. *Rev. Sci. Instrum.* **1996**, *67*, 3238.
(30) Bannwarth, W.; Knorr, R. *Tetrahedron Lett.* **1991**, *32*, 1157.
(31) Charvet, N.; Reiss, P.; Roget, A.; Dupuis, A.; Grunwald, D.; Carayon, S.; Chandezon, F.; Livache, T. *J. Mater. Chem.* **2004**, *14*, 2638.
(32) Bourdos, N.; Kollmer, F.; Benninghoven, A.; Ross, M.; Sieber, M.; Galla, H. J. *Biophys. J.* **2000**, *79*, 357.

stored until utilization. Directly before immersion in thiol solutions, the gold substrates were treated with argon plasma (plasma cleaner, PDC 32G-2, Harrick/USA) for 5 min. All incubations were done from thiol solutions in chloroform or ethanol at room temperature with an overall component concentration of 0.1 mM ($c_{\mathrm{Thiol}} = 0.1$ mM) and a total volume of 2 mL (QSX 301-standard gold quartz crystals, QCM-D measurements) or 4 mL (self-made supports, XPS analysis), respectively. Adequate stock solutions were prepared in deoxygenated chloroform and ethanol; storage was conducted at −20 °C. All incubations were done in weighing bottles to avoid any solvent vaporization. After 24 h thiol incubation time, the gold supports were removed from the thiol solutions, rinsed successively with 10 mL chloroform or 10 mL ethanol and 30 mL water, dried under a nitrogen stream, and directly used for XPS/QCM-D analysis.

All analyzed SAMs densely covered the gold substrates. This was proven by impedance spectroscopy (data not shown). All SAMs had capacitances of ≈1 $\mu\mathrm{F}\cdot\mathrm{cm}^{-2}$, which agrees with reported values for tightly packed *n*-alkane SAMs with an alkyl chain length of ≈16 carbon atoms.[33]

QCM-D Analysis. QCM-D measurements were performed using a Q-Sense E1 system (Q-Sense/Sweden), connected to a peristaltic flow module. The QCM-D device allows time-resolved and simultaneous analysis of resonance frequency shifts (Δf) and dissipation factor changes (ΔD) during mass deposition on shear oscillating quartz crystal surfaces covered with gold electrodes. The Δf and ΔD changes of the fundamental resonance frequency of the quartz shear oscillation ($n = 1$, 5 MHz for QSX 301-Standard Gold quartz crystals, normally omitted due to its spatial sensitivity across the wafer), as well as for harmonics with $n = 3$, 5, ···, 13 were monitored.

Data sets were acquired using *QSoft 401* software (Q-Sense/Sweden). For measurements, SAM-functionalized quartz crystals were mounted in the measurement chamber and constantly overflowed with TBS buffer, pH 7.4, in flow-through. All measurements were accomplished under virtually nonperturbing flow conditions, provided by the Q-Sense flow module with a flow velocity of 0.2 mL liquid per minute at 20 °C. For monitoring SA immobilization, TBS buffer was replaced by SA solution (5 $\mu\mathrm{g}\cdot\mathrm{mL}^{-1}$ SA in TBS, pH 7.4 (1 mL), circular flow). SA immobilizations were followed by rinsing with TBS buffer, ensuring disposal of loosely bound SA from the gold surface. Each SA immobilization experiment (specifiable by its SAM prefunctionalization component ratio and type of solvent) was repeated at least three times from independent sample preparations.

XPS Analysis. XPS spectra were obtained using an AXIS-ULTRA spectrometer (KRATOS, Manchester, UK) in ultrahigh vacuum ($< 10^{-7}$ Pa). Monochromatic Al K_α radiation ($h\nu$ = 1486.6 eV) was used with a 15 kV accelerating voltage and 10 mA filament current (≈500 μm spot diameter). The charge neutralizer was run with a filament current of 1.8 A, a charge balance of 2.3 V, and a filament bias of 1.0 V. For wide survey scans, a pass energy of 160 eV was applied, while high-resolution scans for core-level spectra were acquired with a pass energy of 20 eV. For each sample, XPS spectra were collected by employing a takeoff angle of $\theta = 90°$. For each sample, 3 single measurements were taken at different spots on the sample surface. Between 10 and 20 scans were acquired to get smooth lines and minimize analysis errors. Further data analysis was done using the software *CasaXPS* v 2.2.0 (Neal Fairley/www.casaxps.com). The C1s peak was used as an internal reference, and the binding energy of the signal of the exclusively aliphatic C−C bond was assumed to be 285.0 eV (referenced to its Fermi level). The raw spectra were subsequently smoothed and fitted using mixed Lorentzian−Gaussian line shapes. Quantification was done using the survey spectra and sensitivity factors from the CasaXPS element library (Neal Fairley/www.casaxps.com). Each experiment was repeated three times from independent sample preparations.

Evaluation of QCM-D data—Theoretical basis. QCM-D measures the acoustical response of a shear oscillating, piezoelectric quartz crystal by temporal shifts in the intrinsic quartz crystal shear oscillation resonant frequency (Δf) and changes in dissipation factor (ΔD).[12] The latter represents the inverse of the more common Q-factor[29] and displays the ratio of the energy dissipated in one period of oscillation ($E_{\mathrm{dissipated}}$) and the total energy stored in the system (E_{stored}).

In the case of sufficiently thin layers adsorbed to the oscillating quartz plate, frequency shifts are often directly converted to the mass of material bound to the sensor surface. Hereby, quantification is based on the well-known Sauerbrey relation,[34] which linearly relates frequency shift of the nth overtone (Δf_n) to the immobilized mass ($\Delta m_{\mathrm{Sauerbrey}}$)

$$\Delta m_{\mathrm{Sauerbrey}} = \rho_{\mathrm{film}} h_{\mathrm{film}} \frac{\Delta f_n}{n} \qquad (1)$$

where C_{QCM} denotes the mass sensitivity constant (17.7 $\mathrm{ng}\cdot\mathrm{cm}^{-2}\cdot\mathrm{Hz}^{-1}$ for 5 MHz quartz crystals) and n is the accordant overtone number. However, if the quartz plate is immersed in a Newtonian bulk liquid this relation for thin layers only holds if the adsorbed film can be regarded as an ideally rigid mass layer, homogeneously distributed and with insignificant viscoelastic properties.[35,36] Under these circumstances, the changes in dissipation factor induced by the attached film are marginal and exhibit negligible influence on the mass calculation.[12]

In the case of adsorption of soft layers, internal viscous energy (dissipative) losses might occur during shear oscillation. The shear acoustic wave propagating into and through the film underlies explicit damping, originating from, e.g., hydrodynamically coupled water to the macromolecules constituting the adsorbed layer.[3,9,35−37] This can lead to a theoretical description more complex than the Sauerbrey relation. In QCM-D analysis, the Voight-Voinova representation is used to describe the viscoelastic properties of the layer. The adsorbed film is described by a complex shear modulus leading to analytical expressions for Δf and ΔD changes containing the mass ($m_{\mathrm{film}} = \rho_{\mathrm{film}} h_{\mathrm{film}}$) response as well as the elastic shear modulus (μ) and shear viscosity (η) of the layer.[38] The Voight representation accounts for a frequency (overtone) dependence of normalized Δf shifts as well as for significant changes in ΔD during layer deposition; the effective mass of the film (including surface coupled water) can be calculated in sufficient approximation.

In the present study, SA immobilization experiments monitored by QCM-D were quantified by using the Sauerbrey relation (eq 1) and by modulating the measured Δf_n and ΔD_n changes with the Voight-based representation using *Q-Tools* 3.0.5.198 software (Q-Sense/Sweden). The SA layers are specified by their calculated mass and thickness quantities.

Results

QCM-D Analysis of SA Binding to SAMs. SA binding capacities to thiol SAMs were analyzed via QCM-D. SAMs were formed on gold supports from incubation solutions with varying ratios of thiol I and II (Figure 1). Either chloroform or ethanol was used as solvent. Incubations lasted 24 h to guarantee a tight, ideal thiol packing density.[7]

Figure 2 displays frequency (Δf) and dissipation factor (ΔD) changes as a function of time resulting from SA application to

(33) Porter, M. D.; Bright, T. B.; Allara, D. L.; Chidsey, C. E. D. *J. Am. Chem. Soc.* **1987**, *109*, 3559.
(34) Sauerbrey, G. *Z. Phys.* **1959**, *155*, 206.
(35) Cho, N. J.; Kanazawa, K. K.; Glenn, J. S.; Frank, C. W. *Anal. Chem.* **2007**, *79*, 7027.
(36) Hook, F.; Kasemo, B.; Nylander, T.; Fant, C.; Sott, K.; Elwing, H. *Anal. Chem.* **2001**, *73*, 5796.
(37) Patel, A. R.; Frank, C. W. *Langmuir* **2006**, *22*, 7587.
(38) Voinova, M. V.; Rodahl, M.; Jonson, M.; Kasemo, B. *Phys. Scr.* **1999**, *59*, 391.

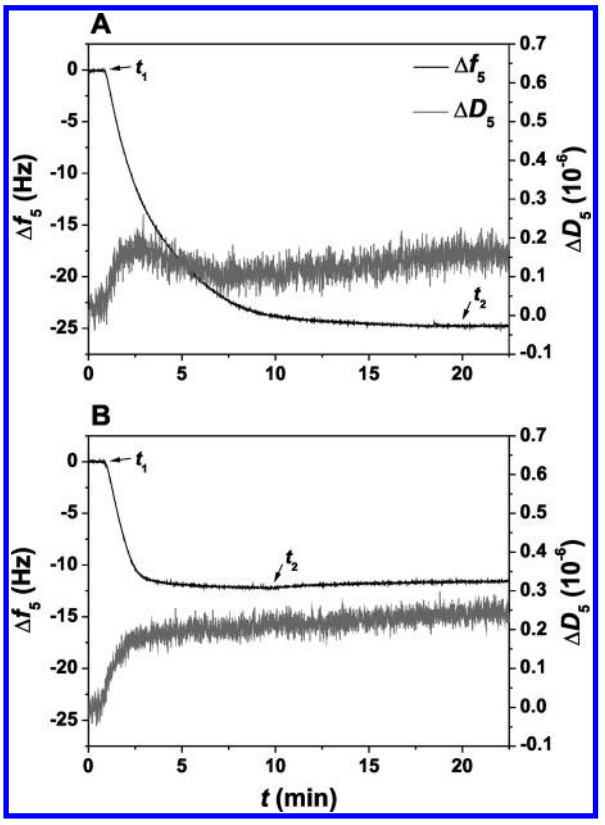

Figure 2. Δf_5 and ΔD_5 data versus time (5th harmonic) resulting from SA application (5 $\mu g \cdot mL^{-1}$) to SAMs prepared with varying molar thiol ratios in solution (24 h incubation). (A) $(n_I/n_{II})_{solution}$ = 50, (B) $(n_I/n_{II})_{solution}$ = 10 000. Incubations were done in chloroform (c_{Thiol} = 0.1 mM).

SAM functionalized Standard Gold quartz crystals. SAMs were formed from thiol solutions in chloroform composed of two different molar ratios of I and II (solution ratio $(n_I/n_{II})_{solution}$). In each case, Δf and ΔD data of the fifth overtone, normalized by the overtone number, are shown (Δf_5 and ΔD_5). For all other harmonics, the normalized Δf_n and ΔD_n changes display congruent traces (data not shown). The moment of SA addition (point "t_1") and the start of buffer rinsing after the completed process (point "t_2") are indicated in the plots.

The QCM-D data in Figure 2 display differing characteristics, primary observable from the varying shifts of resonance frequency. While the incubation with a solution ratio of $(n_I/n_{II})_{solution}$ = 50 (Figure 2A) gives a normalized frequency shift of $\Delta f_5 \approx -25$ Hz, the SA application to a SAM formed from a mixture of $(n_I/n_{II})_{solution}$ = 10 000 (Figure 2B), shows less of a frequency shift ($\Delta f_5 \approx -12$ Hz). 80−90% of Δf changes are achieved after only 3−5 min.

Examination of the dissipation factor (ΔD_5) traces again demonstrates a differing behavior of the two systems. For the SAM formed from a solution ratio of $(n_I/n_{II})_{solution}$ = 50 (Figure 2A), a rapid increase to $\Delta D_5 \approx 0.2 \times 10^{-6}$ can be observed during the first 2 min. The initial rise is followed by a decrease for another 5 min, which then passes into an almost constant plateau, only influenced by a small drift ($\Delta D_5 \lesssim 0.1 \times 10^{-6}$ within 30 min). The ΔD trace resulting from SA application to the SAM formed from a solution ratio of $(n_I/n_{II})_{solution}$ = 10 000 (Figure 2B) shows an initial increase to $\Delta D_5 \approx 0.2 \times 10^{-6}$ (≈ first 2 min), which is followed by the already mentioned drift. No intermediate decrease is observed.

If SA was applied to a SAM formed from a one-component incubation solution exclusively containing thiol I, Δf and ΔD shifts upon SA exposure were negligible ($\Delta f_5 \approx 1$ Hz, $\Delta D_5 \approx 0$, data not shown).

Table 1. Layer Mass (m) and Thickness (h) Resulting from SA Deposition on Different Biotinylated SAMs (N = 3), Specified by Their Component Solution Ratio $((n_I/n_{II})_{solution})^a$

	Sauerbrey		Voight	
	m_{SA} (ng·cm^{-2})	h_{SA} (nm)	m_{SA} (ng·cm^{-2})	h_{SA} (nm)
$(n_I/n_{II})_{solution}$ = 50	413 ± 16	3.6 ± 0.2	415 ± 16	3.6 ± 0.1
$(n_I/n_{II})_{solution}$ = 10 000	199 ± 10	1.7 ± 0.1	202 ± 15	1.8 ± 0.2

[a] Calculations were done via Sauerbrey and Voight method. An effective SA layer density of ρ_{film} = 1150 kg m^{-3}[39] was assumed.

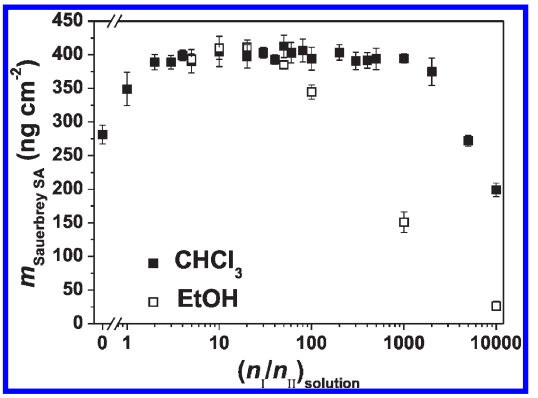

Figure 3. Immobilized mass quantities $m_{Sauerbrey\ SA}$ resulting from SA application (5 $\mu g \cdot mL^{-1}$) to SAMs formed with different solution ratios $(n_I/n_{II})_{solution}$ (24 h incubation, c_{Thiol} = 0.1 mM). The SAMs were formed in chloroform or ethanol.

SA layer mass quantities resulting from SA application to biotinylated SAMs as shown in Figure 2 were calculated both via Sauerbrey[34] (cf. eq 1, Δf_5 (n = 5, i.e., 25 MHz)) and Voight method[38] (the data of the fifth, seventh, and ninth overtone were used). The data of three independent measurements were used (N = 3). Additionally, the layer thicknesses were calculated, assuming an effective SA film density of ρ_{film} = 1150 kg·m^{-3}.[39] Table 1 lists the corresponding data. Both calculations yield the same mass quantities, thus denoting that the linear proportionality approximation between frequency shift and adsorbed mass holds in the present case. Thereby, SA applications to SAMs formed from a molar solution ratio of $(n_I/n_{II})_{solution}$ = 50 lead to a significantly higher SA mass/layer thickness immobilized on the SAM surface than the exposure to the SAMs formed from incubations with less amount of thiol II ($(n_I/n_{II})_{solution}$ = 10 000).

A more detailed view on the SA binding behavior of binary SAMs is given in Figure 3. SAMs were formed from 24 h incubations with varying thiol solution ratios $(n_I/n_{II})_{solution}$. Either chloroform or ethanol served as thiol solvent. Figure 3 shows the accumulated masses ($m_{Sauerbrey\ SA}$) onto the SAMs specified by $(n_I/n_{II})_{solution}$.

In the case of chloroform as thiol solvent, a SA layer mass of $m_{Sauerbrey\ SA} \approx 400$ ng·cm^{-2} is observed over a broad range of thiol solution ratios ($2 \leq (n_I/n_{II})_{solution} \leq 1000$). Higher fractions (e.g., one-component system thiol II ($(n_I/n_{II})_{solution}$ = 0)) as well as lower fractions of thiol II ($(n_I/n_{II})_{solution}$ > 1000) display a reduced amount of immobilized mass.

For ethanol, SAMs were formed from incubation solutions of different representative component ratios (Figure 3). Comparison of SA layer mass quantities resulting on SAMs formed in ethanol to SAMs prepared in chloroform shows characteristic differences.

(39) Hook, F.; Ray, A.; Nordn, B.; Kasemo, B. *Langmuir* **2001**, *17*, 8305.

Table 2. Elemental Percentages of SAM I and SAM II as Revealed by Wide-Scan Survey XPS Analysis[a]

peak position	SAM I		SAM II	
	Calculated (%)	Measured (%)	Calculated (%)	Measured (%)
C (C1s, BE = 285.0 eV)	88.89	85.4 ± 0.2	74.42	66.8 ± 1.1
N (N1s, BE = 400 ± 1.0 eV)	-	-	9.30	11.9 ± 0.1
S (S2p, BE = 162.5 ± 1.0 eV)	5.56	1.9 ± 0.3	4.65	3.4 ± 0.3
O (O1s, BE = 532.3 ± 1.0 eV)	5.56	12.7 ± 0.5	11.63	17.9 ± 1.3

[a] The theoretical values of the elemental percentages (chemical structure) and the respective electron binding energies (BEs) are also depicted.

While a molar solution ratio of $(n_I/n_{II})_{solution} = 10$ in ethanol led to a SA layer mass of $m_{Sauerbrey\ SA} \approx 400$ ng·cm^{-2} (similar to chloroform), a solution ratio of $(n_I/n_{II})_{solution} = 100$ caused an already decreased binding capacity. For $(n_I/n_{II})_{solution} = 1000$ in ethanol, significantly less material was immobilized ($m_{Sauerbrey\ SA}$ = (151 ± 15) ng·cm^{-2}). Regarding the lowest amount of thiol II in the incubation solution ($(n_I/n_{II})_{solution} = 10\,000$), SA addition resulted in only marginal mass deposition ($m_{Sauerbrey\ SA}$ = (27 ± 7) ng·cm^{-2}).

XPS Study of SAMs. SAMs formed from thiol solutions (c_{Thiol} = 0.1 mM, 24 h) in chloroform and ethanol were investigated by XPS. Wide-scan spectra (electron binding energy (BE) range 0−1200 eV) and high-resolution scans for the core-level spectra of carbon (C1s) were collected for the one-component SAMs (SAM I and SAM II) as well as for SAMs formed from binary thiol mixtures with varying thiol solution ratios $(n_I/n_{II})_{solution}$.

Chloroform, One-Component SAMs (SAM I and SAM II). Table 2 summarizes the elemental percentages of SAM I and SAM II formed in chloroform obtained by wide scan survey analysis (peak intensity analysis of C1s, N1s, O1s, and S2p signals; spectra not shown). Additionally, the calculated molecular percentages (chemical structure) are given. For all elements of the one-component SAMs, only moderate agreement of calculated and measured data was obtained. In particular, the measured fractions of O deviate to larger values for both SAMs. The reverse was observed for the percentage of measured S.

Any chlorine peak intensities originating from residual solvent were absent. In all cases, signals from the gold substrate (Au4f, Au4d, Au4p) could be identified (data not shown).

Figure 4 shows the C1s core-level spectra taken from SAM I and SAM II. For both thiols, a pronounced superposition resulting from the varying chemical environments of the corresponding carbon atoms is visible. For thiol I, the C1s spectrum was decomposed into three different carbon positions with varying intensities (CPS - counts per second). The corresponding spectrum of thiol II was deconvoluted into six individual peaks. The different signals used for the deconvolution were adapted from NMR spectra of the pure components (data not shown); all electron binding energies (BEs) of the different types of carbon peak positions were derived from the literature.[40] The positions C−O and C−N were unified since rather similar BEs must be expected (for detailed information about the deconvolution procedure, see Supporting Information).

Table 3 lists the carbon BE positions used in the deconvolution procedure as well as the percentages of the different C species determined from the peak intensities of the C1s core-level spectra of SAM I and SAM II (cf. Figure 4). The theoretical percentages following from the chemical structure were added. Similar to the wide scan analysis, exact agreement of calculated and measured data could not be achieved. However, the percentages of the different C species approximated by the signal deconvolution resemble the calculated values.

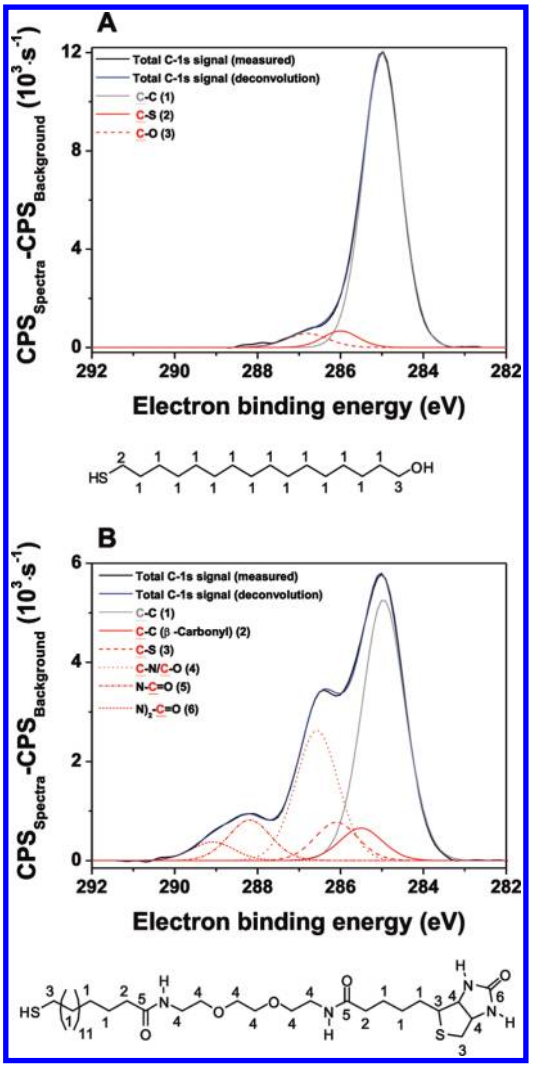

Figure 4. C1s core-level spectra of SAM I (A) and SAM II (B). The deconvolution into the different carbon peaks and the sum of the single carbon peaks are also depicted. For peak positions and the respective results of the peak intensity analysis, see Table 3.

Chloroform, Binary SAM Systems. SAMs formed by 24 h incubations in chloroform with varying thiol solution ratios ($1 \leq (n_I/n_{II})_{solution} \leq 500$) were analyzed in the same way as the one-component SAMs. For all SAMs, the elemental percentages were derived from the wide scan survey spectra. The C1s core-level spectra were used to identify the percentages of the different C species.

From these data, the thiol ratios in the SAMs, $(n_I/n_{II})_{SAM}$, were calculated in two different ways: Calculation method A: The measured ratios of N and C percentages (N/C ratios), derived from the wide scan spectra, were used. Since N is unique for thiol

(40) Beamson, G.; Briggs, D. *High Resolution XPS of Organic Polymers*; Wiley: Chichester (England), 1992.

Table 3. Percentages of the Different Carbon Species of SAM I and SAM II as Revealed by C1s Core-Level Analysis[a]

C1s peak position	SAM I		SAM II	
	calculated (%)	measured (%)	calculated (%)	measured (%)
C−C (BE = 285.0 eV)	88.90	91.1 ± 0.2	50	50.4 ± 0.7
C−C (β-carbonyl) (BE = 285.7 ± 0.2 eV)	-	-	6.25	6.4 ± 0.2
C−S (BE = 286.3 ± 0.2 eV)	5.55	4.0 ± 0.2	9.38	7.1 ± 0.3
C−N/C−O (BE = 286.7 ± 0.2 eV)	5.55	4.9 ± 0.1	25	25.4 ± 0.4
N−C═O (BE = 288.3 ± 0.2 eV)	-	-	6.25	7.3 ± 0.5
$N)_2$−C═O (BE = 289.2 ± 0.2 eV)	-	-	3.13	3.4 ± 0.2

[a] The theoretical values (elemental formula) and the respective BEs are also depicted.

II, the measured N percentage in binary systems reflects the fraction of thiol II in the SAM. The deviations between measured and calculated elemental percentages identified for the one-component SAMs were considered in the binary systems (for a detailed description, see Supporting Information).

Calculation method B: The measured ratios of the aliphatic (C−C, C−H) carbon percentages (BE = 285.0 eV) and the sum of all residual (nonaliphatic) carbon percentages ($C_{aliphatic}/C_{nonaliphatic}$ ratios) were identified from the C1s core-level spectra. Thereby, the percentages of the individual C species were approximated by a deconvolution of the corresponding C1s signals (cf. Figure 4, Table 3). Since the percentage of non-aliphatic carbon peak intensities is significantly higher in thiol II compared to thiol I, the corresponding percentage in binary systems reflects the fraction of thiol II in the SAM (a graphic evolution of the C1s signal intensity with BE > 285.0 eV due to the enrichment of thiol II in the system can be found in the Supporting Information). The $C_{aliphatic}/C_{nonaliphatic}$ ratios were used to identify the SAM ratios $(n_I/n_{II})_{SAM}$. Similar to "Calculation method A", the SAM ratios were determined on the basis of the data obtained for the one-component systems (SAM I and SAM II, cf. Table 3; for a detailed description, see Supporting Information).

Figure 5 shows the SAM ratios $(n_I/n_{II})_{SAM}$ of all analyzed SAM substrates as a function of the corresponding solution ratio $(n_I/n_{II})_{solution}$ in chloroform. The parameter $(n_I/n_{II})_{SAM}$ was identified using "Calculation method A" (N/C ratio) and "Calculation method B" ($C_{aliphatic}/C_{nonaliphatic}$ ratio), respectively. In all cases, large differences between $(n_I/n_{II})_{SAM}$ and $(n_I/n_{II})_{solution}$ are demonstrated. The fractions of biotinylated thiol II in the SAMs are distinctly increased if compared to the corresponding fractions within the solution. For example, a solution ratio of $(n_I/n_{II})_{solution} = 100$ leads to a 37 fold lower surface ratio of $(n_I/n_{II})_{SAM} = 2.7 \pm 0.2$.

For solution ratios of $(n_I/n_{II})_{solution} \leq 100$, an exact agreement between both calculation methods can be observed. For $(n_I/n_{II})_{solution} > 100$ the consistency decreases. The reason is that only marginal N1s signal intensities were detected above the inelastic scattering background, meaning that the XPS detection limit was reached. Accordingly, the C1s signal deconvolution must be considered to be increased erroneously. Nevertheless, both calculation methods agree quantitatively for the major part of the analyzed thiol systems.

Ethanol. Different SAMs formed from ethanolic incubation solutions (c_{Thiol} = 0.1 mM, 24 h) were investigated via wide-scan survey ((BE) range 0−1200 eV) analysis (data not shown). Similar to the measurements in chloroform, deviations of elemental fractions in the one-component SAMs were analyzed and compared to the corresponding calculated values (data not shown). Again, the N/C ratios measured for SAMs formed from binary solutions (specified by $(n_I/n_{II})_{solution}$) were used to calculate the SAM ratios $(n_I/n_{II})_{SAM}$ (see Supporting Information, "Calculation method A").

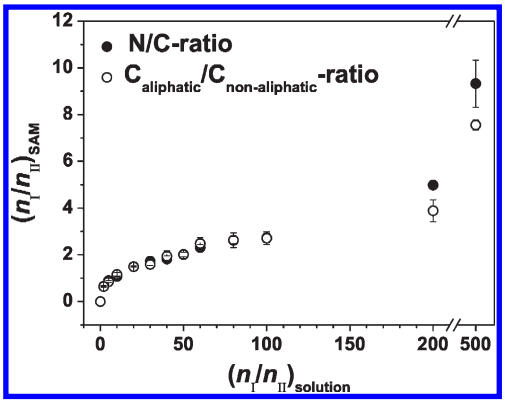

Figure 5. Thiol SAM ratios $(n_I/n_{II})_{SAM}$ as a function of the corresponding ratios in incubation solution ($(n_I/n_{II})_{solution}$). The ratios $(n_I/n_{II})_{SAM}$ were derived from the XPS wide-scan survey spectra (N/C ratio analysis, "Calculation method A") and from the C1s core-level spectra ($C_{aliphatic}/C_{nonaliphatic}$ ratio analysis, "Calculation method B"). Incubations were done in chloroform (c_{Thiol} = 0.1 mM, 24 h).

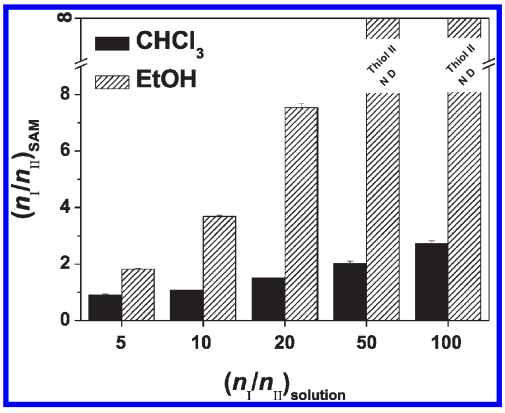

Figure 6. Comparison of SAM ratios $(n_I/n_{II})_{SAM}$ of SAMs formed from different solution ratios $(n_I/n_{II})_{solution}$. Either chloroform or ethanol were used as thiol solvent (c_{Thiol} = 0.1 mM, 24 h). The $(n_I/n_{II})_{SAM}$ were calculated via N/C ratio analysis (Calculation method A). For solution ratios of $(n_I/n_{II})_{solution} = 50$ and $(n_I/n_{II})_{solution} = 100$ in ethanol, the percentages of nitrogen were below the detection limit of XPS (N D ≡ Not Detectable).

Figure 6 shows the calculated SAM ratios $(n_I/n_{II})_{SAM}$ for different solution ratios $(n_I/n_{II})_{solution}$. The corresponding results obtained for incubations in chloroform are also depicted (cf. Figure 5). Significant differences are visible: In ethanol, SAMs with distinctly smaller fractions of thiol II were obtained. For example, SAMs formed with solution ratios of $(n_I/n_{II})_{solution} = 20$ in ethanol yield a surface ratio of $(n_I/n_{II})_{SAM} = 7.5 \pm 0.2$, while corresponding incubations in chloroform led to $(n_I/n_{II})_{SAM} = 1.5 \pm 0.1$. Ethanolic incubations with solution ratios of $(n_I/n_{II})_{solution} \geq 50$ led to SAMs with fractions of thiol II below

the detection limit of XPS. No N1s signal could be detected in the wide-scan spectra. Thus, the SAM ratio $(n_I/n_{II})_{SAM}$ could not be determined.

Discussion

QCM-D Analysis of SA Binding to SAMs. In the present study, SA binding characteristics to biotinylated SAMs composed of thiols I and II (Figure 1) were analyzed by QCM-D. The Δf and ΔD dependencies obtained for SA binding on a SAM formed from a solution ratio of $(n_I/n_{II})_{solution} = 50$ show a region of simultaneous decrease in resonance frequency and dissipation factor, e.g., from ≈ 2 min onward in Figure 2A. Such a temporal decrease of both Δf and ΔD has also been demonstrated in recent QCM-D studies, where SA layers were arranged on biotinylated lipid bilayers[9,39] or biotinylated SAMs.[22] In our case, the absolute ΔD changes detected are of low magnitude and effected by a typical ΔD drift vs time (cf. Figure 2). However, the temporal decrease can be reliably identified from the ΔD trace.

Surface films causing low dissipation exhibit a high rigidity. A decrease in ΔD must be attributed to a film transformation, i.e., a stiffening process of the layer to a more rigid state.[9,22,39] In the case of SA surface films, the stiffening is ascribed to the formation of lateral SA−SA interactions, mediated by specific contact regions between the individual protein molecules. SA is able to form crystal-like structures of monomolecular thickness at biotinylated interfaces (2-D crystallization). Within intact 2-D crystal regions, the SA molecules cover approximately 50−60% of the surface, thus forming structures with rather high water content.[41−45] Former QCM-D studies quantified the mass of solid supported SA crystalline arrangements (including hydrodynamically coupled water) via Sauerbrey method to approximately 450−550 ng cm^{-2}.[9,22,39]

The mass of SA layers on SAMs formed from a molar solution ratio of $(n_I/n_{II})_{solution} = 50$ in chloroform ($m_{layer} \approx 415$ ng cm^{-2}, Table 1) is in good agreement with the mentioned QCM-D studies.[9,22,39] Application of the Sauerbrey relation[34] and the Voight representation[38] gave consistent results, showing that the Sauerbrey approximation for rigid layers is sufficient for mass calculation. Considering the maximal SA surface capacity in a monolayer arrangement (2-D crystalline ≈ 50−60%)[43,44] and the molecular weight of SA ($M_{SA} \approx 55$ kDa), a molecule surface density of ≈2.5 × 10^{12} molecules·cm^{-2} can be determined for a complete SA layer. From this, a projection area of ≈25 nm^2 results for a single SA molecule, in line with reported values.[43]

Using an effective density of $\rho_{layer} = 1150$ kg m^{-3} (approximated value, based on a 1/1 mass ratio of SA ($\rho \approx 1300$ kg m^{-3}) and water ($\rho \approx 1000$ kg m^{-3}))[39] results in a layer thickness of $h_{SA} \approx 3.6 \pm 0.14$ nm. This agrees with former studies based on, e.g., ellipsometry.[46,47] Considering the dimensions of a SA molecule (≈5.4 × 5.8 × 4.8 nm^3),[43] the calculated thickness seems to be underestimated. However, it is important to note that the calculated layer thickness is related to the SAM. Before SA immobilization, the biotin moieties and ethylene glycol spacers of thiol II protrude from the hydroxyl-terminated background of thiol I, and contribute to the SAM thickness. For example, for one-component SAMs of (*N*-(8-biotinyl-3,6-dioxa-octanamidyl)-functionalized thiols a contribution of approximately 1.5−2.0 nm was reported.[24,47,48] After SA deposition, a fraction of biotin groups is buried in the SA binding pockets (insertion depth ≈ 1.4 nm),[43] while residual biotin moieties are located in possible SA layer vacancies. Thus, the biotin groups have to be regarded as a part of the SA surface film, not of the underneath SAM. Furthermore, the calculated film thickness implies a homogeneous SA layer, where surface defects and porosity of the real system are neglected. Other uncertainties originate from the estimated water content of the SA layers. Considering these criteria, the approximated SA layer thickness of ~3.6 nm appears reasonable with respect to the molecular size of SA.

In the case of SA layer formation on SAMs formed from a solution ratio of $(n_I/n_{II})_{solution} = 10\,000$ (Figure 2B), two important differences can be observed. First, mass (thickness) calculations of deposited SA show less immobilized material on the transducer surface compared to the complete 2-D crystalline coverage (cf. Table 1). Again, the thickness is calculated using an effective density of $\rho_{layer} = 1150$ kg m^{-3}. Note that this value must be classified as an approximated value. The intrinsic fraction of trapped water (i.e., the protein/water mass ratio) within SA films showing only partial coverage might be different from that of a complete, crystalline SA layer,[12,37] leading to variations in the effective density. However, the overall trend of a reduced SA binding capacity to the SAMs can be concluded.

Second, the Δf and ΔD traces do not show the indication for 2-D crystallization. The film stiffening process is less pronounced, emphasizing the observation originating from the mass determination: SA layers, which do not show a maximal protein surface density, naturally have fewer SA−SA interactions within the surface film and exhibit less compact structures.

It should be mentioned that one-component SAM I inhibits SA binding. The SA binding detected in the binary systems can be ascribed to the specific SA-biotin interaction.

The data shown in Figure 3 confirm the dependence between the SA layer formation quantity and the solution ratio $(n_I/n_{II})_{solution}$. High fractions of biotinylated thiol II in the incubation solution lead to a reduced SA binding capacity due to sterical hindrance between adjacent biotin groups.[2,15,20,24,26]

Regarding the SA binding behavior on SAMs formed from solutions with low fractions of thiol II, a more detailed interpretation has to be given. For a thiol SAM on gold exhibiting a $(\sqrt{3}\times\sqrt{3})R30°$ periodicity, a molecule density of ≈4.5 × 10^{14} molecules·cm^{-2} can be calculated.[7] Above a molecule surface density of ≈2.5 × 10^{12} molecules·cm^{-2} was calculated for a complete SA layer. Assuming an ideal SA packing on the SAM where each biotin binds a SA molecule, a SAM ratio of $n_{diluent\ thiol}/n_{biotinylated\ thiol} \approx 180$ would be sufficient for the assembly of a complete SA 2-D crystal. The optimal ratio is decreased by various effects which influence the described optimal interaction efficiency:[7,49] (1) SA exhibits two binding sites for biotin on either side of the molecule. Enhanced fractions of biotin thiol in the monolayer lead to increased probability of SA binding via both binding pockets. (2) A nonrandom or heterogeneous thiol distribution induces less biotin accessibility for the binding pockets. (3) Microscopic and nanoscopic gold surface irregularities (e.g., grain structures, etch pits, or pinholes) lead to mismatched thiol assemblies in the SAM.

(41) Scheuring, S.; Muller, D. J.; Ringler, P.; Heymann, J. B.; Engel, A. *J. Microsc.* (*Oxford*) **1999**, *193*, 28.
(42) Schief, W. R.; Edwards, T.; Frey, W.; Koppenol, S.; Stayton, P. S.; Vogel, V. *Biomol. Eng.* **1999**, *16*, 29.
(43) Hendrickson, W. A.; Pahler, A.; Smith, J. L.; Satow, Y.; Merritt, E. A.; Phizackerley, R. P. *Proc. Natl. Acad. Sci. U.S.A.* **1989**, *86*, 2190.
(44) Darst, S. A.; Ahlers, M.; Meller, P. H.; Kubalek, E. W.; Blankenburg, R.; Ribi, H. O.; Ringsdorf, H.; Kornberg, R. D. *Biophys. J.* **1991**, *59*, 387.
(45) Coussaert, T.; Volkel, A. R.; Noolandi, J.; Gast, A. P. *Biophys. J.* **2001**, *80*, 2004.
(46) Reiter, R.; Motschmann, H.; Knoll, W. *Langmuir* **1993**, *9*, 2430.
(47) Kim, D. J.; Koo, K. K. *J. Ind. Eng. Chem.* **2004**, *10*, 920.
(48) Schmidt, A.; Spinke, J.; Bayerl, T.; Sackmann, E.; Knoll, W. *Biophys. J.* **1992**, *63*, 1385.
(49) Yang, G. H.; Liu, G. Y. *J. Phys. Chem. B* **2003**, *107*, 8746.

Taking these arguments into account, the QCM-D data of SA binding events to SAMs formed from incubations in ethanol and chloroform can be considered (Figure 3). In the case of chloroform, the complete SA binding capacity is preserved for incubation solutions exhibiting remarkably low fractions of thiol II. In fact, the thiol solution ratio being sufficient for maximal SA immobilization quantity ($(n_I/n_{II})_{solution}$ = 1000) ranges two decades below the optimal SAM ratio stated in the literature for similar thiol systems ($(n_{diluent\ thiol}/n_{biotinylated\ thiol})_{SAM} \approx 10$).[15,20] In addition, a thiol solvent effect is revealed. SAMs formed of binary thiol solutions in chloroform demonstrate higher SA binding capacities compared to SAMs prepared from the same solution ratio $(n_I/n_{II})_{solution}$ in ethanol. Former studies on binary SAMs based on, e.g., XPS or impedance spectroscopy illustrated varying adsorption affinities for different thiols on gold depending on structural characteristics (e.g., alkyl chain length, headgroup character) and nature of incubation solvent.[17,24,27] Considering our QCM-D data, an elevated adsorption efficiency of thiol II compared to thiol I was observed, and the effect is more pronounced in chloroform.

XPS Study of SAMs. The focus of the XPS study is the correlation between the used thiol solution ratios for SAM formation ($(n_I/n_{II})_{solution}$) and the resulting SAM ratios $(n_I/n_{II})_{SAM}$ after 24 h incubation.

Concerning the wide-scan analysis of the one-component SAMs, deviations of calculated and measured data must be expected due to the oriented thiol assembly in the monolayer. The influence of inelastic photoelectron scattering (inelastic electron mean free paths)[50] and the mean element specific distance from the SAM surface[24] lead to the attenuation of S2p signals. In particular, this effect was observed for SAM I, which solely contains covalently linked sulfur at the Au interface. The elevated percentage of oxygen is due to physisorbed water on top of the SAM, which is often reported to remain on hydrophilic SAM surfaces.[51−53] For this reason, the calculation of $(n_I/n_{II})_{SAM}$ of SAM formed from binary solution was done by using the carbon and nitrogen signal intensities which are less influenced by the described effects.

The gold signals detected in all wide-scan spectra confirm the fact known in literature that the organic thiol layer exhibits surface defects.[26,54]

No signal intensities originating from chlorine could be detected in the spectra of SAMs prepared from chloroform, meaning that no residual solvent was existent. This fact enabled the rather complex deconvolution of the C1s core spectra presented in Figure 4. The total C1s signal intensity can be exclusively assigned to the thiol molecules, since no contribution from chloroform must be expected. We do not claim our signal decomposition to be the only one possible. However, in the present case and under the constraints of our procedure (see Supporting Information) the decomposed signal intensities resemble the calculated expectations (Table 3). Furthermore, application of "Calculation method B" for the identification of $(n_I/n_{II})_{SAM}$ in binary SAM systems led to similar results as "Calculation method A" (Figure 5), giving evidence that the chosen deconvolution is applicable at least in the present case.

For ethanolic incubations, a thiol surface ratio calculation based on core-level spectra analysis was omitted. As reported earlier,[51] all SAMs contained residual ethanol and thus C1s signal intensities not belonging to the thiol molecules. The trapped solvent leads to C1s signal fine structures, which could not be reasonably decomposed in separated C1s contributions.

The XPS results emphasize the interpretation originating from the QCM-D data. Incubations in chloroform lead to an elevated adsorption efficiency of thiol II leading to enhanced fractions of biotinylated thiol II on the gold surfaces compared to the corresponding portions in solution. This effect ensures a complete SA coverage of the thiol monolayers even if only marginal amounts of thiol II are present during the 24 h incubations for SAM formation. In the case of ethanolic incubations, the SAMs contained distinctly fewer fractions of thiol II. The XPS results demonstrate in line with the QCM-D study that the thiol system used here is subjected to a strong solvent effect. For ethanolic SAM formations, moderately enhanced adsorption efficiencies of biotinylated thiols in similar thiol systems are described in the literature:[20,24] In this study, we show that the adsorption efficiency of thiol II is strongly enhanced in chloroform.

Deviations between thiol ratios in solution $(n_I/n_{II})_{solution}$ and on gold surfaces $(n_I/n_{II})_{SAM}$ after long incubations (≥1 day) can be explained in terms of thermodynamic aspects of the adsorption process.[16−18,27] For ethanol, the moderately enhanced adsorption efficiency of thiol II can be attributed to a lower solubility of the biotinylated component compared to thiol I, i.e., a thermodynamic control.[20] The significantly increased effect in chloroform may be a result from a higher solubility difference of thiol I and thiol II in chloroform. These conditions would elevate the (thermodynamic) absorption affinity of thiol II to the gold and explain the strong solvent effect observed in our study.

Conclusion

In our study, SA layers were prepared on binary SAMs consisting of 16-mercapto-1-hexadecanol (thiol I) and *N*-(8-biotinyl-3,6-dioxa-octanamidyl)-16-mercaptohexadecanamide (thiol II). Our findings demonstrate differing protein binding behavior depending on the fraction of biotin moieties within the preformed SAM. The SA layer surface density correlates with the fraction of thiol II in the system. For appropriate amounts of biotin, the QCM-D data indicate the formation of complete SA monolayers. SA film mass quantities could be calculated via the Sauerbrey method.[34] During protein immobilization, a film stiffening, originating from a (partially) 2-D crystalline SA arrangement, was observed. Excessive or insufficient fractions of thiol II lead to SA layers with noncomplete coverage. These layers feature fewer intermolecular contact regions and fewer indications of film stiffening. The fraction of thiol II in the SAM showed a dependence on two major aspects: (1) the portion of thiol II in the incubation solution used for SAM formation, and (2) the distinct influence of the choice of solvent. The adsorption efficiency of thiol II is elevated, and the effect is significantly more pronounced in chloroform compared to ethanol. Considering these aspects, the SAM surface composition can be controlled.

Acknowledgment. Prof. Dr. H. Eckert is gratefully thanked for providing the XPS device being essential for the presented study. We further thank The"Fond der Chemischen Industrie", the "NRW Graduate School of Chemistry" and the "Deutsche Forschungsgemeinschaft" (DFG) for financial support.

Supporting Information Available: Additional information as described in the text. This material is available free of charge via the Internet at http://pubs.acs.org.

(50) Powell, C. J.; Jablonski, A. *J. Phys. Chem. Ref. Data* **1999**, *28*, 19.
(51) Sprik, M.; Delamarche, E.; Michel, B.; Rothlisberger, U.; Klein, M. L.; Wolf, H.; Ringsdorf, H. *Langmuir* **1994**, *10*, 4116.
(52) Wirde, M.; Gelius, U.; Nyholm, L. *Langmuir* **1999**, *15*, 6370.
(53) Tielens, F.; Costa, D.; Humblot, V.; Pradier, C. M. *J. Phys. Chem. C* **2008**, *112*, 182.
(54) Voicu, R.; Boukherroub, R.; Bartzoka, V.; Ward, T.; Wojtyk, J. T. C.; Wayner, D. D. M. *Langmuir* **2004**, *20*, 11713.